Design and development of low-power output solar chimney power plant

Ashenafi Tesfaye(MSc)[a*],Solomon T/mariam(PhD)[b],Tewodros walle(Msc)[c]

[a]*Institute of Technology/University of Gondar, Gondar,Ethiopia*
[b]*Addis Ababa institute of technology/Addis Ababa university, addis Ababa,Ethiopia*
[c]*Addis Ababa institute of technology/Addis Ababa university, addis Ababa,Ethiopia*

Keywords:
Solar energy
Solar chimney power plant
Optimum chimney height
Solar collector
Natural convection

A B S T R A C T

Among the conversion of Solar energy resource into useful power source technology like PV cell is the most significant system worldwide. Recently, a solar chimney power plant (scpp) is proposed to be a cost-effective mechanism for the production of electrical energy on a large scale for the future. In the SCPP system solar air collector, chimney tower and turbine are the three essential main components. In this study solar chimney power plant is investigated for a maximum power output of 30 kW. The optimization of geometry for each component and flow characteristics of air temperature inside the collector is analysed. As a result for 30 kW power output the selected optimized dimensions: chimney height, collector diameter, chimney diameter and collector height (distance between the edges of collector and the ground) are estimated to be 15m, 15m, 0.2m and 0.2m respectively. For a fixed chimney diameter and collector height, an increase in the height of the chimney raises the power output up to a certain optimum height, an increase in chimney height beyond the optimum point results an energy loss due to pressure drop along the chimney will start to dominate the energy rise due to the stack effect. The model developed is scaled down to a chimney height of and collector diameter of with maximum power output of 32 W. In the experiment under investigation the characteristics of the temperature inside the collector throughout the day was studied by the varying height of the collector above the ground from 0.17 m up to 0.4 m. The temperature of the fluid is Minimum when the collector height is 0.4 m and maximum at 0.17 m. The result obtained for a temperature difference between collector exit and collector inlet from the comparison of the experimental and simulated model is in a good agreement under a certain condition. So, the implementation of large scale solar chimney power plant as rural electrification is feasible with the potential to provide electrical energy throughout the day for the desired potential.

* *Corresponding author.* Tel.: +251-912-36-68-56
E-mail address: ashenafites1234@gmail.com

1. Introduction

The cause for the serious environmental problem is primarily an increase in global fossil fuel consumption and the rapid growth of the global economy.

Today, fossil fuels are the primary fuel sources and are still widely used for major electricity generation around the world. According to the report of (Renewable and Agency, 2017),the energy consumption for electricity production worldwide is projected to increase up to 2040 G.C.

Nomenclatures

A	: Area $[m^2]$
D	: Chimney diameter [m]
E_{eff}	: Effectiveness of coefficient
h_{c1}	: Glazing height from ground at entrance[m]
h_{c2}	: Glazing height from ground at exit[m]
H	: Chimney height[m]
Δp_{tot}	:Total pressure difference [Pascal]
P	: Power [W]
Q	: heat gain $[W/m^2]$
T_a	: Temperature of the air inside the collector [K]
$\boldsymbol{T_{pm}}$	**:** Mean plate temperature [K]
Tp	: Average temperature of a plate [K]
Δx	: Thickness of the absorber plate[m]
V	: Flow velocity $[m/s]$
V_{bed}	:Volume of bed$[m^3]$

Greek Symbols

α:absorption coefficient
β:coefficient of volumetric thermal expansion,
η:Efficiency
μ:dynamic coefficient
f:friction factor
v:viscosity
τ: transmittance
γ:isentropic constant

Subscripts

1, 2, 3, 4:Position along plant (as in Fig. 2)
chim :chimney
$Coll$:collector
gz:glazing
abs :absorber
$abs, surf$: Absorber surface area
Pb:pebble
f:fluid(air)
tur:turbine
Sol:solar
lift: Power required to lift air in the chimney
SCPP: solar chimney power plant

Most of the developing countries have high solar radiation resource(Wetstone *et al.*, 2016).For example, in Ethiopian it is estimated that the a daily solar radiation potential varies between (3.2 -6.4) $kwh\ /\ m^2$ as shown in figure 1.However, Electricity generation is highly dependent on hydropower plant.

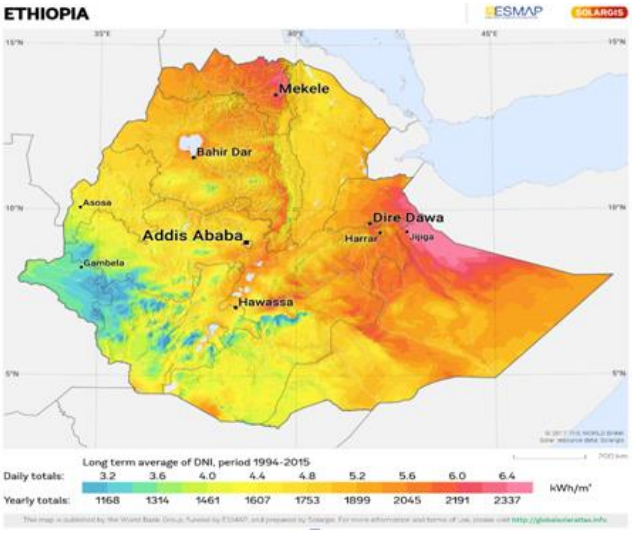

Figure 1:Ethiopian Solar resource map (Renewable and Agency, 2017)

According to report by (Renewable, Program and Final, 2015) in Ethiopia's electricity generation composition from a renewable source was 93.1%. The majority share (92.5%) comes from hydro generation.

The solar chimney power plant is a naturally driven power generating system. It converts solar energy first into thermal energy then into kinetic energy finally into electrical energy. It combines the concept of solar air collectors and a central updraft chimney to generate a solar induced convective flow which drives turbines to generate electricity.

In this research small-scale solar chimney power is studied by aiming to electrify clinic located remote area with the load demand up to 30 kW electrical power.

This study is significant in terms of introducing electricity generation from solar radiation by air convection. Electricity generation from solar radiation by air convection works when the air beneath the collector get heated, its density decreases.

The buoyance force and the pressure difference between the top and base of the chimney pushes the air upward. Part of this heat power converts to a mechanical energy by the axial flow turbine mounted at the base of the chimney. This study combines three basic concepts GHG effect, collector effect and chimney effect to produce power. This system can be adopted in a place where wind speed is lower.

2. Literature review

Studies conducted by (Pasumarthi&Sheriff, 1998) showed that the collector performance can be modified by extending the collector base and by introducing an intermediate absorber. The modification help in increasing air temperature and mass flow rate inside the chimney resulting in higher power output. In 2010,(Koonsrisuk, Lorente and Bejan, 2010),Studied the effect of tower area change in a solar chimney power plant was using CFD technology. The study showed that the tower area change affects the efficiency and the mass flow rate through the plant. It was found out from their study that although velocity increases at the top of a convergent tower, the mass flow rate remains similar as that of a constant area tower. For a divergent tower design, velocity increases near the base of the chimney and the maximum kinetic energy also occurs at the base of the chimney.

(Hamdan, 2010), performed an analytical model and a thermodynamic study of steady airflow inside a solar chimney. He used a simplified Bernoulli's equation combined with fluid dynamics and ideal gas equation using EES solver to predict the performance of the solar chimney power plant. The study showed that the height and diameter of the solar chimney are the most important design variables for solar chimney power plant. However, collector area has small effect on second-law efficiency but strong effect on harvested energy. (Ming *et al.*, 2016), established a simple analysis on the air flowing through the solar chimney power plant and also studied the thermodynamic cycle of the solar chimney power plant . They also developed a mathematical model of ideal and actual cycle efficiencies for medium-sized and large-sized solar chimney power plant. Accordingly the result of their study showed that the ideal cycle efficiency and actual efficiency of standard Brayton cycle corresponding to medium scale solar chimney power generation system are 1.33% and 0.3% respectively, while the ideal efficiency of large scale SC system with chimney height 1000 m is 3.33%, while the maximum value of the actual efficiencies is 0.9%.The results from their work used as a theoretical guideline for designing and building a commercial-size solar chimney power plant in China.(Backström, Gannon and Backstro, 2000), presented an air standard cycle analysis of the solar chimney power plant to show the relationship between different variable to evaluate its performance.

(Pretorius, 2007), Investigate the optimization and control of large scale solar chimney power plant by developing a numerical simulation model. The effects of ambient wind speed, temperature, lapse rates and night time energy storage system temperature variation on plant performance are examined. The work indicated that, the collector reflectivity, emissivity, ground surface absorptivity highly affects performance of the plant.

(Backström, Gannon and Backstro, 2000), analyzed the cycle of a chimney with the simple air standard cycle. Considering a simple air standard cycle as it determines the upper performance limits of the ideal solar chimney power plant. In 2002 (Backström, Gannon and Backstro, 2002),developed simple thermodynamic cycle analysis that includes system losses. Gannon and Von Backström (2000 & 2002) analysis and investigate, the two most important variables in terms of power output in the solar chimney power plant are the chimney height and the solar collector temperature rise, this fundamental relationship is found by developing simple complete air standard cycle.

2.1 Air standard cycle of SCPP cycle and the surrounding air expansion.

The air standard cycle of SCPP and the sir surrounding has the similar principle with air standard cycle of an air standard gas turbine ideal power cycle. In the SCPP cycle analysis compression takes place in the environment as shown in figure 3, this makes the cycle different from gas turbine cycle where the compression takes place in the system. In an ideal gas

turbine power the expansion process entirely takes place inside the turbine. However in SCCP, It takes place first in the turbine in process 2-3, and the remaining takes along the chimney system. The power required lift the air into chimney exit is considered to be a loss the plant.

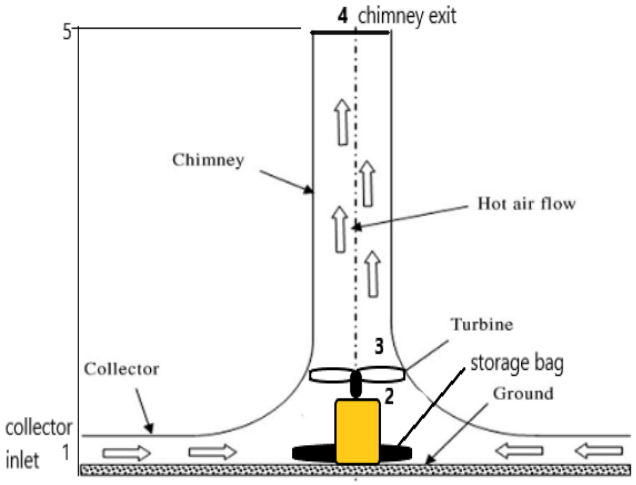

Figure 0: solar chimney power plant with generator and storage unit.

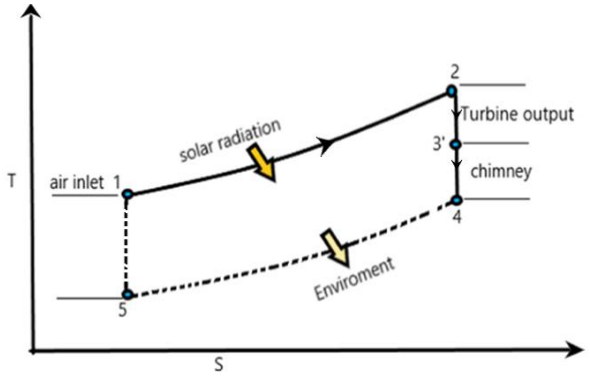

Figure 3: T-S diagram of solar chimney power plant air standard cycle

Cooling process 4-5 is not inside the power plant. The exhaust air is mixed with the ambient air at state 5 and cooled back to state 1.

The total heat input is;

$$Q_i = \dot{m} \times (h_2 - h_1) = \dot{m} C_P (T_2 - T_1) \quad \textbf{(1)}$$

The Expansion energy to lift the air up to state 4:

$$P_{lift} = \dot{m} \times g \times H_{chim} \quad (\mathbf{2})$$

The energy exchange is isentropic, since the friction and heat transfer are negligible. Then the value of enthalpy (Δh) can be equated to the amount of air that has descended down in the atmosphere after having been cooled from chimney exit temperature. So, the enthalpy change in the chimney becomes;

$$\Delta h = g \times \Delta H_{chim} = Cp \times (T_1 - T_5) \quad (\mathbf{3})$$

Then the turbine shaft power becomes;

$$P_{shaft} = \dot{m} \times Cp \times (T2 - T3) - \dot{m} \times Cp \times (T_1 - T_5) \quad (\mathbf{4})$$

3. Design of Solar Chimney Power Plant: A case study

Detail study of SCPP is performed through combining, a theoretical design of technical parameters and simulation of the possible system main component using CFD tools. In order to select geometrical configuration for desired 30 kW power out MATLAB software is used as an optimization tool. For the analysis of temperature and thermal characteristics inside the collector, ENERGY 2d is used as computational fluid dynamics (CFD) tool, it is also used to simulate the temperature variation in all dimension of Collector sides.

The actual prototype shown in figure3 is designed and developed to generate power out of 30 $watt$maximum.So, after theoretical design, the geometry of the prototype is modelled using CATIA V5 and simulated using MATLAB.

Figure 4:Solar chimney power plant at test site,AAiT campus.

In the technical design of the solar chimney power plant, equation is developed by considering the basic concept of conservation of energy, thermodynamic, momentum and continuity equation.

i. Momentum equation

Figure 4 shows the instantaneous fluid flow through the area

beneath the collector.

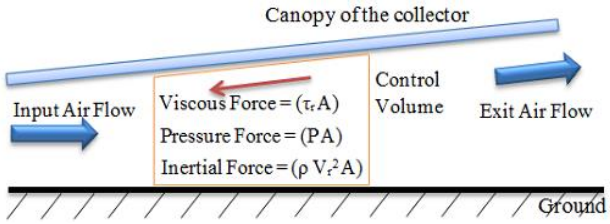

Figure 4: The force that acts inside the bottom of the collector

Balance of forces of air flow inside the collector can be obtained by applying Newton's second law for partial control volume:

$$\frac{\partial(\rho V_r^2)}{\partial r} = -\frac{\partial P}{\partial r} + \frac{\partial \tau_r}{\partial r} + \rho g \qquad (5)$$

Where:$\frac{\partial P}{\partial r}$: is the free streams of pressure gradient and shear stress,$\tau = \mu \frac{\partial V}{\partial r}$

ii. Continuity equation

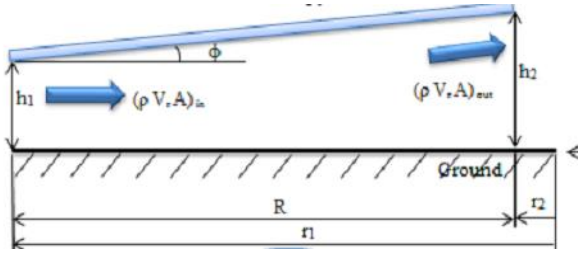

Figure 6: Radial section of collector

The continuity equation of the collector is written as;

$$(\rho_1 V_r A_{COLL})in = (\rho_2 V_r A_{COLL})out \qquad (6)$$

iii. Energy Conservation

The total energy per area of the collector is the sum of;

Heat gain into the glazing = heat lost from the glazing

Heat gain into the absorber = heat lost from the absorber

Heat gain into the fluid = heat lost from the fluid

Heat gain into the ground = heat lost from the ground

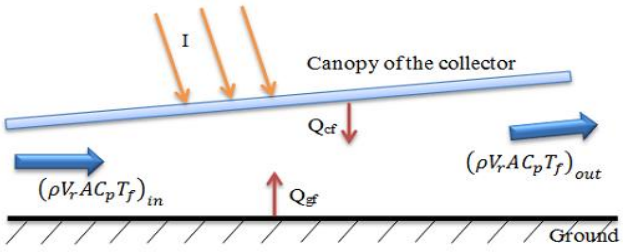

Figure 7: Energy balance diagram for SCPP system.

In solar chimney power plant the flow of the fluid is due to natural convection. In the meanwhile, ENERGY 2D can model SCPP as a natural and mixed convection by considering buoyancy source term. Natural convection is when the fluid is driven by local density difference while mixed convection flows occurs when the convection of a fluid is driven by both a pressure gradient and buoyancy forces.

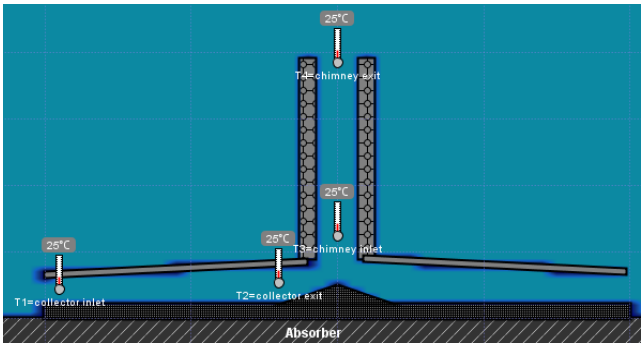

Figure 8: Thermal boundary condition setting

ENERGY 2D is used to investigate the characteristics of the fluid flow inside the collector as shown in figure 8. For the simulations, steady state analysis is selected by creating an environment of updraft solar chimney power plant in the interface of ENERGY 2D.

Mathematical modelling

In order to calculate the available power output of the plant an assumption will be made initially for pressure extraction ratio P_3/P_2. The collector inlet pressure P1 is assumed as Patm=0.77 bar (atmospheric pressure at inlet @$T_1 = 25℃$), since the plant is operated open to the environment pressure variation between the collector inlet and collector exit are neglected. By considering the number stationed in figure 2 all the parameters are equated as follow.

The **collector exit temperature** is found from energy equation;

$$q'' A_{gz} = \frac{1}{2}\dot{m} \times (v_2^2 - v_1^2) + \dot{m} \times Cp(T_2 - T_1) \qquad (7)$$

According to (Koonsrisuk and Chitsomboon, 2013) frictional effect is ignored since the velocity in this region is quite low. Because the flow is in the very low Mach number regime, the kinetic energy contribution can be neglected.

Then the above equation will be re-written as:

$$q'' A_{gz} = \dot{m} Cp(T_2 - T_1) \qquad (8)$$

This shows that the mass flow rate is inversely proportional to the collector temperature rise, Since the mass flow rate is assumed to be constant, then collector area can be found from (Koonsrisuk and Chitsomboon, 2013) equation.

$$T_2 = T_1 + \frac{q'' A_{gz}}{\dot{m} Cp} \quad (9)$$

Heat flux q'' incident on the surface of the glazing

$$q'' = (\alpha \times \tau) \times G_r - U_t \times \Delta T \quad (10)$$

The work extraction process at the turbine is assumed to be an isentropic process, Temperature of air at the entrance of chimney or turbine exit (T_3) can be calculated from the equation below;

$$T_3 = T_2 \left(P_3/P_2\right)^{\frac{\gamma-1}{\gamma}} \quad (11)$$

Then the **pressure P_4 at the chimney exit** can be found from the following equation;

$$P_4 = P_1\left(1 - \left(\frac{g * H_{chim}}{Cp * T_1}\right)^{Cp/R}\right) \quad (12)$$

From ideal gas constant the **density** of each state can be written as;

$$\rho = \frac{P}{RT} \quad (13)$$

In order to determine the density at the chimney outlet the temperature at that state should be known; According to the (Backström, Gannon and Backstro, 2000) equation of **temperature at chimney exit $T4$**becomes;

$$T_4 = T_3 - g \times \frac{H_{chim}}{Cp} \quad (14)$$

Now recall that the above parameter are computed by the assumed value of pressure P_3,so this result has to be validated by equation developed by (Backström, Gannon and Backstro, 2000) for actual P_3.

Pressure at the chimney inlet or turbine outlet;

$$P_{3actual} = P_4 + 0.5 \times (\rho_3 + \rho_4) \times g \times H_{chim} + \left(\frac{\dot{m}}{A_{gz}}\right)\left(\frac{1}{\rho_4} - \frac{1}{\rho_3}\right) \quad (15)$$

The tower (chimney) converts the heat-flow produced by the collector into kinetic energy (convection current) and potential energy (pressure drop at the turbine). The density difference caused by the temperature rise in the collector works as driving force.

The lighter column of air in the tower is connected with the surrounding atmosphere at the base (inside the collector) and at the top of the tower, and thus acquires lift. The pressure difference Δp_{tot} is produced between tower base (collector outlet) and the ambient;

Pressure difference can be written as;

$$\Delta p_{tot} = g \times \int_0^{Hchim} (\rho_2 - \rho_4) dH \quad (16)$$

The **pressure difference** can be re-written as;

$$\Delta p_{tot} = g \times (\rho_2 - \rho_4) \times H_{chim} \quad (17)$$

The useful driving pressure is;

$$P_t = \Delta p_{tot} - P_f \quad (18)$$

Where P_f=frictional pressure drops

Then the **velocity at the chimney entrance V_2** can be found from (Zhou, Xiao, *et al.*, 2010);

$$V_2 = \frac{G(\tau \times \alpha) \times A_{gz} - \beta(\Delta T_a \times A_{gz})}{\rho_{air} A_{chim} c_p (\Delta T)} \quad (19)$$

Then, $\Delta T_a = (T_{pm} - T_1)$

i. Mean plate temperature (T_{pm})

$$T_{pm} = T_1 - \frac{Q_{useful}}{A_{gz} \times \beta \times F_R} \times (1 - F_R) \quad (20)$$

ii. Collector Heat removal factor (F_R)

$$F_R = \frac{\dot{m} \times C_P}{A_{gz} \times \beta}\left(1 - \exp\left(\frac{A_{gz} \times \beta \times F'}{\dot{m} \times C_P}\right)\right) \quad (21)$$

The theoretical **power extracted** by the turbine can be determined from the energy equation and Gibbs relation from classical thermodynamics:

$$P_{out} = \eta_{tur} \times P_t \times V_2 \times A_{gz} \quad (22)$$

So, in order to calculate the theoretical power output using eq. (22), the solution procedure shown if fig. (9) Has to be followed.

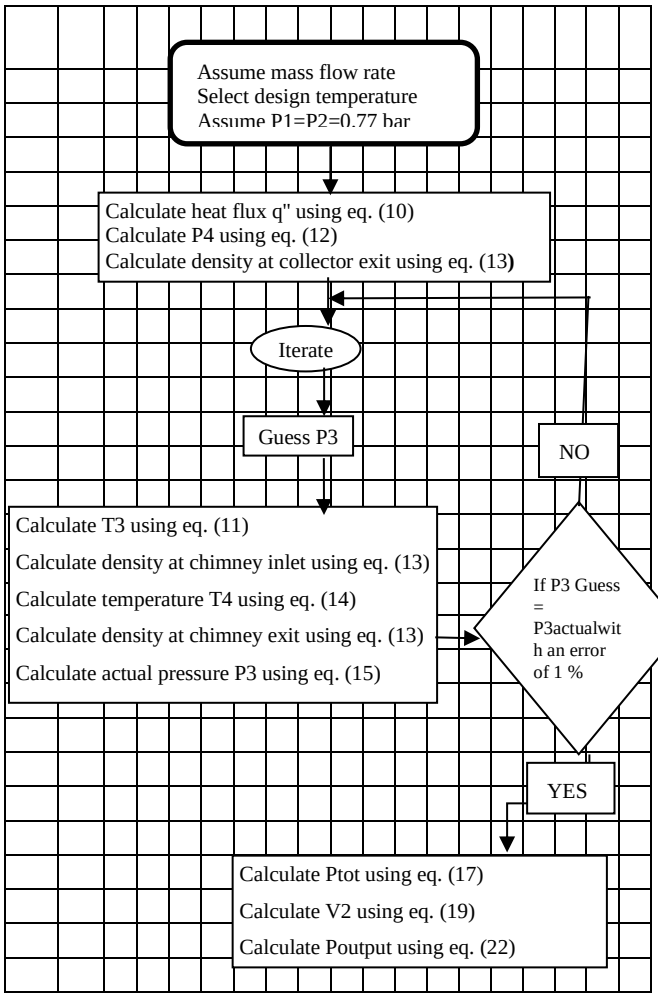

Figure 9: Flow chart for power output calculation procedure.

Result and discussion

In this study, MATLAB is used to study the optimum geometrical size of main component of SCPP that provides maximum power output. In the analysis the influence of different parameter on the power output has been investigated as shown in the following sections

1. Power output vs diameter of glazing (collector)

The simulation is investigated for five different power output with same fixed parameter of chimney diameter, collector height from the ground and various chimney height as shown in figure 10.it is observed that increasing the diameter of a chimney will results an increase in total power output as a result of increase in collector exit temperature at indicated fixed- parameters. Additionally, in order to achieve the designed power output of 30 kW from the plant, a chimney height must be more than 10 meters for an indicated fixed parameter.

Table 3: Geometry selection for 30kW for power output

Options	Geometry				
	$Hchim$	$hc1$	$Dcoll$	$Dchim$	$Power(kW)$
1	3 m	200 mm	30 m	200mm	15 kW
2	6 m	200 mm	28 m	200mm	30 kW
3	9 m	200 mm	22 m	200mm	30 kW
4	12 m	200 mm	16 m	200mm	30kW
5	15 m	200 mm	13 m	200mm	30kW

2. Height of chimney versus power output

The simulation shown in figure 11 was conducted by varying the height of chimney and diameter of collector while fixing diameter of chimney and collector height from the ground at 0.2 m each.

The simulation shown in figure 11 is useful in order to show the optimum chimney height that provides the maximum power Output for a certain collector diameter, chimney height and collector height from the ground.

For the case study under consideration, conclusion has been made on the selection of the geometrical size of chimney height and collector diameter for the desired power output of 30 kW based on the factor like, cost of construction, construction simplicity and site area coverage for the plant. So, it is concluded that option three (3) is a better option for the application of 30 kW power output, with chimney height of 17 m and 17 m of collector diameter as shown in table 4.

Moreover, by keeping the fixed parameters and increasing the chimney height to 45 m and the collector diameter of 25 m more than 350 kW power output can be achieved.

On the other hand, using the selected geometry of chimney height and collector diameter as a fixed parameter and making a change on the fixed parameters will result more power output as shown in the figure 12, thus increasing the chimney diameter from 0.2 meter up to 1 meter will result in increased more than 4 kW.

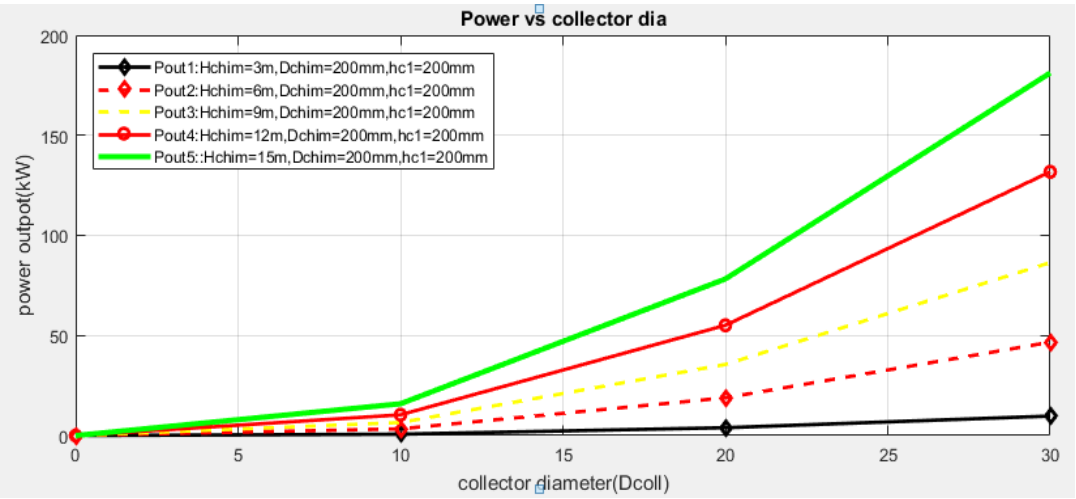

Figure 10: collector diameter vs. power output

Table 4: Chimney height selection for $30kW$

options	Geometry				Power (kW)
	$Dchim$	$Dcoll$	$Hchim$	$hc1$	
1	200 mm	5 m	60 m	200 mm	21 kW
2	200 mm	10 m	28 m	200 mm	30 kW
3	200 mm	17 m	17 m	200 mm	30 kW
4	200 mm	20 m	9 m	200 mm	30 kW
5	200 mm	25 m	7 m	200 mm	30 kW

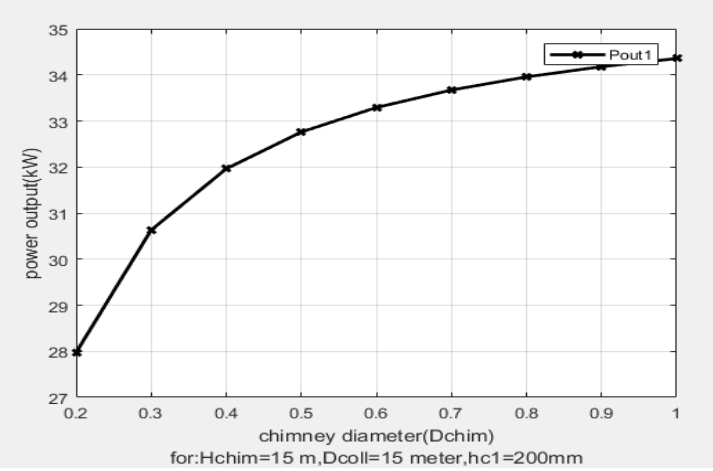

Figure 12: chimney height vs. power at various chimney diameters

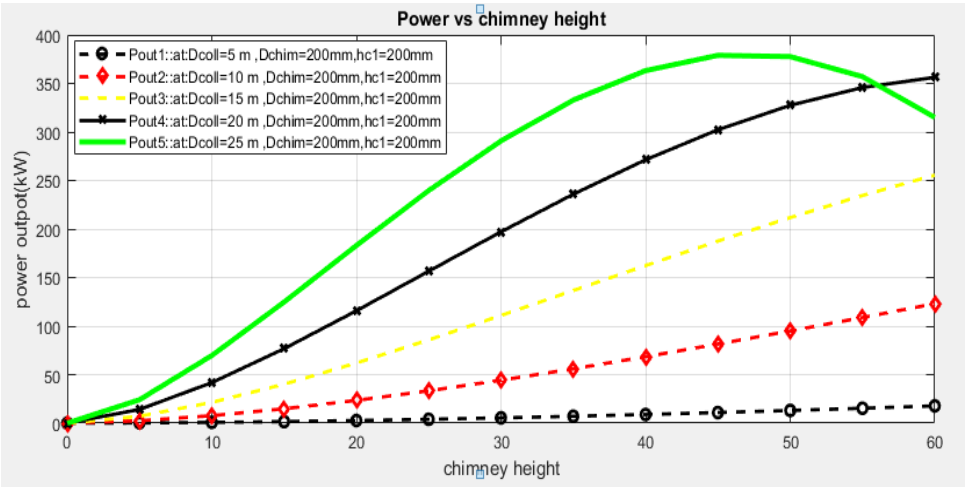

Figure 11: Height of a chimney vs. power output

Table 5: Optimum chimney height for different chimney diameter and collector diameter

	Dcoll	*Dchim*	hc1	Optm. Hchim	Max. Pout.
1	5 m	0.2 m	200 mm	600 m	800 kW
2	10 m	0.4 m	200 mm	500m	2 MW
3	15 m	0.6 m	200 mm	370 m	4.7 MW
4	20 m	0.8 m	200 mm	370 m	8 MW
5	25 m	1.0 m	200 mm	370 m	14 MW

Figure 13, Simulates the optimum chimney height that provides optimum power output at fixed height of the collector from the ground at the same time with varying chimney diameter and collector diameter. The investigation was carried out by running the chimney height up to $600\,m$ .The optimum chimney height for selected geometrical set are listed in as shown in table 5.

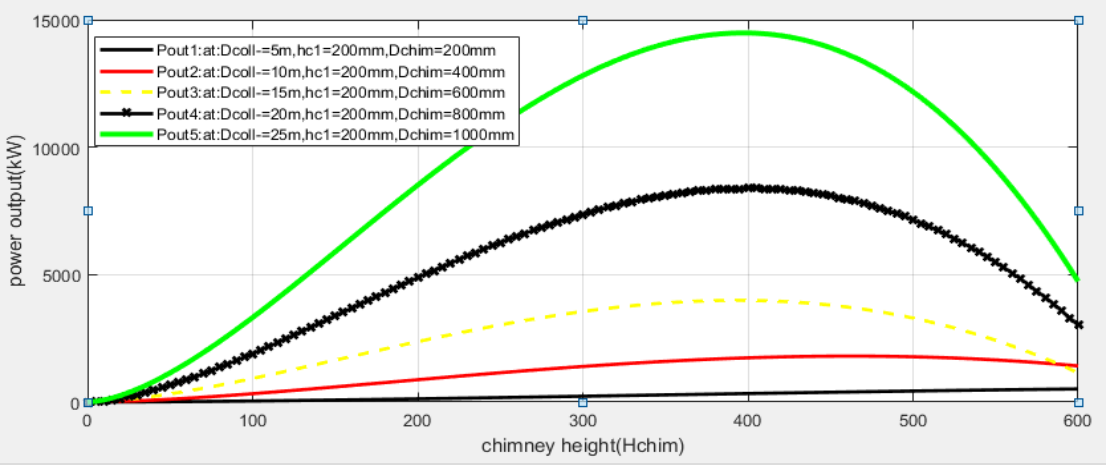

Figure 13: Optimum chimney height for various collector diameters.

Therefore, increasing the chimney height greater than the indicated value shown in table 5, results in a reduction of power output at the indicated fixed parameters, this is caused by the total frictional pressure drop in the chimney (draft tube) system.

3. MATLAB result for Experimental set up

3.1 Height of chimney versus power output

According to the analysis shown in figure 14, increasing the height of the chimney above 62 meters at fixed collector height from the ground (hc1=170mm), diameter of the chimney (Dchim=160mm), diameter of the collector (Dcoll=2 m) will result power output reduction, the decrease in the power is caused by domination of a frictional pressure along the chimney(draft tube).When a chimney height reaches 107 m the power output equal to zero means frictional pressure loss is equal to useful driving pressure. Therefore, for the indicated fixed parameters shown the optimum chimney height for useful energy production is 58 m.

Table 6: Geometry specification for a model developed

No	Parameter	Value	units
1	Chimney height	3 m	H_{chim}
2	Collector diameter	2 m	D_{coll}
3	Chimney diameter	160 mm	D_{chim}
4	Collector height from the ground	170-400 mm	h_{c1}

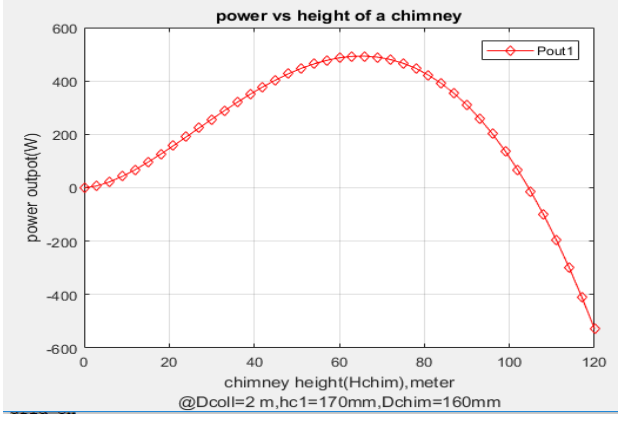

Figure14: Power versus chimney height

For this particular study under consideration, the developed experimental solar chimney power plant is constructed with 3-meter chimney height and 2 meter collector diameter which provides a maximum power output of 32 W as shown in the above figure.

3.2 Collector diameter vs. power output

Following the simulation shown in figure 15, increasing the diameter of the collector up to 3 m will increase the power output of the plant to 9 kW at the indicated parameters collector height from the ground, diameter of the chimney and height of chimney fixed at 170mm, 160mm and 3 m respectively.

Whenever the collector diameter exceeds more than 5 m the rate of power production increases more than twice, this also gives the chimney power plant is more economical for larger scale electrical power generation

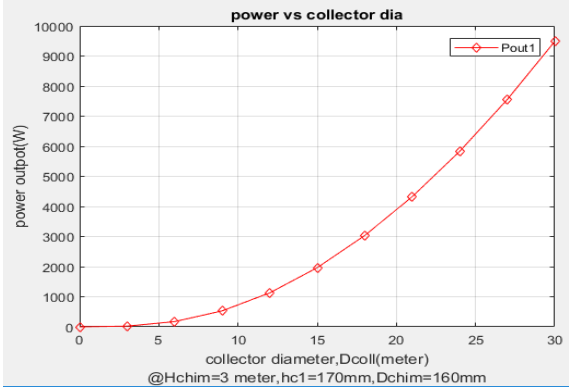

Figure 15: power output versus collector diameter idea that solar.

3.3 Pressure (Pt) versus height of the chimney

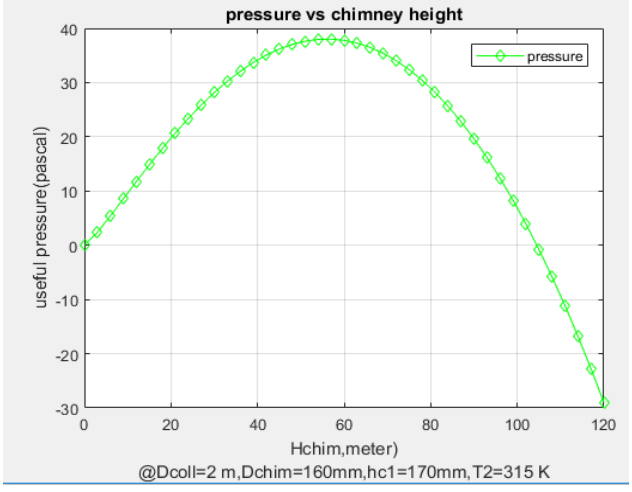

Figure 16: Useful Pressure versus chimney height

At a fixed parameter of chimney diameter, collector diameter, collector exit temperature and height of the collector from the ground of 160 mm, 2 m, 315 K and 170 mm respectively. The useful pressure (Pt) increases until the chimney height reaches 58 meters, beyond this height of the chimney the pressure tend to dramatically dropdown due to the cumulative effect of frictional pressure loss. At a fixed parameter useful pressure is zero when the chimney height reaches 103 meter this result in zero power output of the solar chimney power plant. So, the maximum allowable chimney height for this designed solar chimney power plant is 58-meter unless if the is no change in the fixed parameter as shown in figure 16.

4. Temperature simulation using ENERGY 2D

For this study, the boundary condition for the temperature simulation is shown in the figure 8. Background temperature of working fluid is25℃.In the figure 17, the variation of working fluid temperature throughout the day at collector inlet, collector exit, chimney inlet and chimney exit are simulated. In simulation conducted using ENERGY 2D tool, solar-radiation data and sun angle is influenced following the data obtained from source. So, according to the simulation the temperature of collector exit varies from 31℃ – 43℃ throughout the day, the minimum temperature reading was recording during morning time of 10:00 am and maximum temperature was recorded during the mid-day at 12:38 PM.

4.2 Temperature throughout the day at height of the collector**, hc1=170 mm**

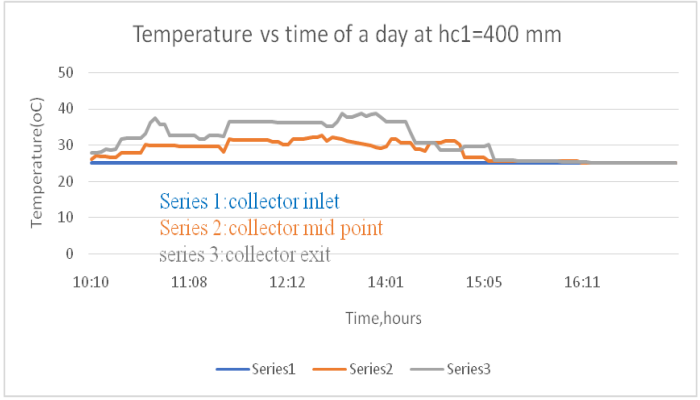

Figure 18: Temperature simulation at hc1=400

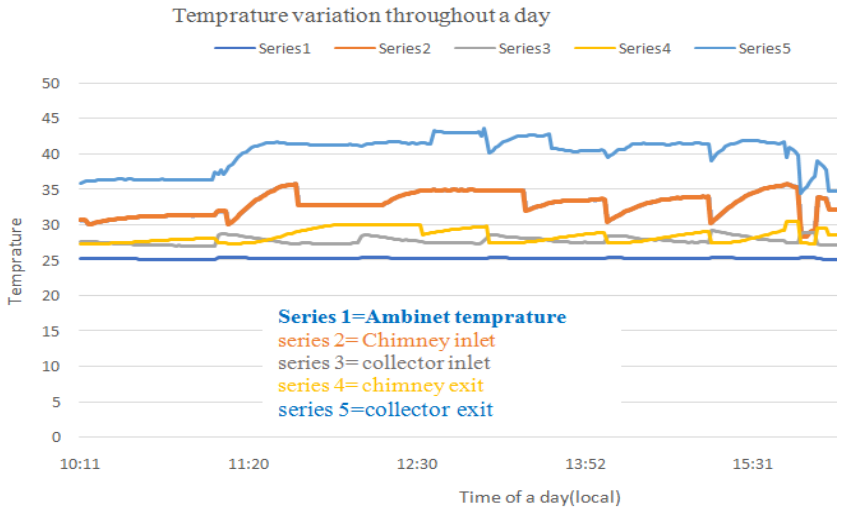

Figure 19: Temperature simulation at hc1=170mm

4. Actual prototype temperature test result

4.1 Temperature throughout the day at height of the collector, hc1=170 mm

In the experiment test result shown in figure 19, the temperature variation through the day was taken for three days in May 16/18, May 22/18 and May 23/18. The data was recorded for more than 6 hours per day for three different days; an average was taken for every 5-minute recording due to the instability of the weather condition. The maximum collector exit temperature reading of 41.7℃ was recorded at mid-day at $12:44:00\ PM$.

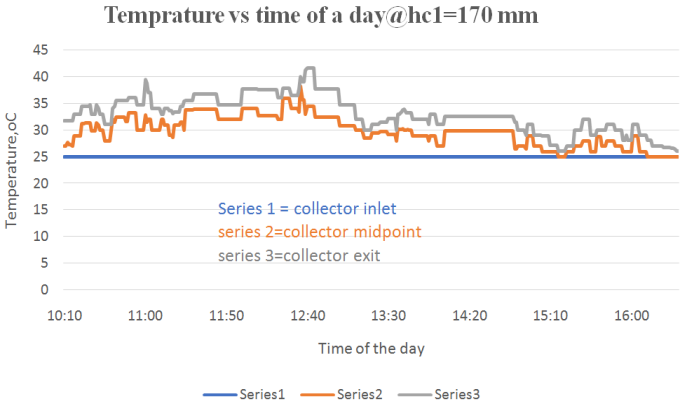

Figure20: Actual prototype temperature result throughout a day at@hc1**=170mm**

The temperature result shown in the figure 18 is recorded by increasing the height of the collector from the ground to 400 mm. The maximum collector exit temperature 38.8℃ is recorded during 13:04 PM and minimum collector exit temperature of 25℃ is recorded during 16:10 PM.

4.3 Comparison between temperature at different collector height from Ground($hc1$)

In the experiment the collector exit temperature reading is taken for collector height of the 170 mm and 400 mm from the ground. In figure 20, it is clearly seen that the collector exit temperature is lower throughout the day for collector height of 400 mm and higher for a 170 mm collector height. So, it can be concluded that whenever the height of the collector from the ground is higher, the collector exit temperature will be lower at indicated fixed geometrical configurations.

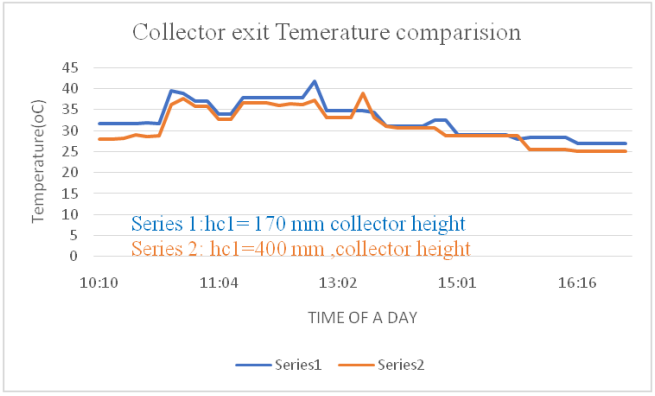

Figure 21: Collector exit temperature comparison for different collector height from ground

5. Validation of experimental result with simulated result

5.1 Temperature difference Vs Time of the day

In the figure 21, the comparison of experimental model and mathematical model are conducted by taking temperature difference of collector exit and collector inlet throughout the day. So, the temperature difference of the experimental model increases from 10:00 AM up to 12:44 PM resulting minimum and maximum temperature difference of 6℃ upto 17 ℃ respectively, then the temperature difference drops down from 12:50 PM up to 13:00 PM.On the other hand, the mathematical model temperature difference increases from 10:00 AM up to 15:00 PM, then it starts to drop down up to 15:10 PM.

Generally, the results show that after 12:44 PM the characteristics of the two models have a variation in collector exit temperature difference. For the actual experiment under consideration, the temperature of the collector exit was lower during the afternoon as a result of the cloudiness in the sky, in the simulation this factor was not considered following solar data collected.

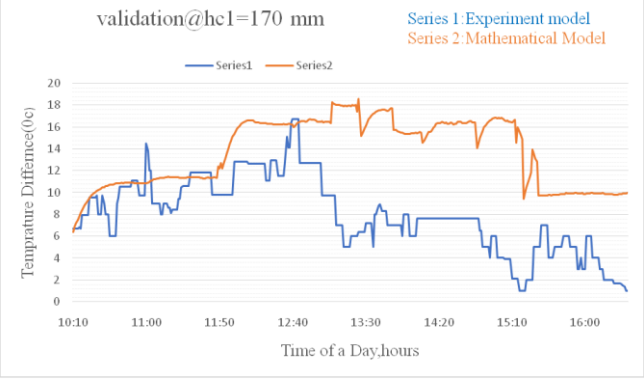

Figure 22: temperature difference for experiment vs simulation model

5.2 Power output vs time of the day

The power output for both models depends on the temperature difference throughout the day. So, the power output of the actual experiment varies from $8\,watt - 32\,Watt$, maximum power output was recorded during the mid-day at $12{:}44\,PM$ and minimum at$15{:}19\,PM$. While, the simulated power output varies from$20\,Watt - 34\,watt$, maximum at $13{:}20\,PM$ and minimum at$10{:}10\,AM$.

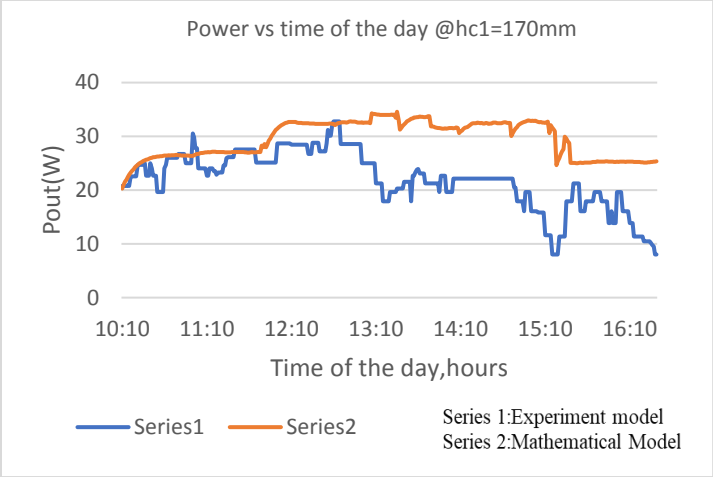

Figure 23: Power output for actual experiment vs mathematical model

Generally, for the actual experiment, the flow characteristics of power output is unstable as a result of collector exit temperature variation throughout the day, this is as a result of environmental and geographical condition at test site as shown in figure 23.

6. Efficiency of the collector (Glazing)

The collector efficiency is the ratio of heat output from the collector per solar radiation (G) received per unit area of a collector and expressed as shown below.

$$\eta_{coll} = \frac{\dot{Q}}{G \times A_{COLL}} = \frac{\dot{m} \times Cp \times (\Delta T)}{G \times A_{COLL}} \qquad \text{eq(23)}$$

According to(Koonsrisuk and Chitsomboon, 2013),the Heat output$\dot{Q}$ under steady conditions can be expressed as a product of the mass flow rate $\dot{m}$, the specific heat capacity Cp of the air and the temperature difference between collector inflow and outflow ($\Delta T = Tout - Tin$).The curve shown in the figure 23 represents characteristics of efficiency with respect to solar radiation input through a day.

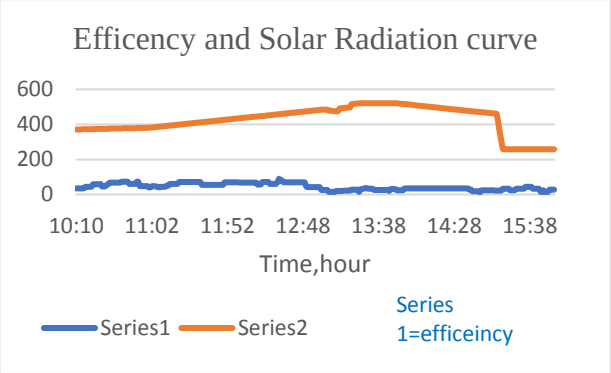

Figure 24: Efficiency and Solar radiation curve

The efficiency in the above figure is analysed at a collector area, collector height from the ground and chimney diameter of 3.14 m^2 , 0.17 m and 0.16 m respectively.

According to this study the efficiency of the collector cannot be certainly concluded that whenever solar radiation increases the efficiency increases or vice versa. So, it is concluded that efficiency of the collector is dependent of temperature difference throughout the day. Eq. (25) also gives the idea that however solar radiation increases the efficiency of the collector does not exceed a collector optical property of transmittance-absorptance. So, increases an in efficiency of the collector does not always mean there is high solar radiation in the site.

$$Q = \tau\alpha \times G \times A_{COLL} - \beta(\Delta Ta) \times A_{COLL} \quad \text{eq(24)}$$

$$\eta_{coll} = \tau\alpha - \frac{\beta(\Delta Ta)}{G} \quad \text{eq(25)}$$

For the fixed geometrical configuration and material selected the average efficiency of the collector is around 67.4%.

Conclusions

Following the result of the simulation and experiment the following conclusion are drawn.

i. Increasing the collector height from 0.17mupto 0.4 m above the ground reduces the collector exit temperature, resulting reduced power output. The higher the height of the collector above the ground the lower the temperature inside collector.

ii. Increasing the height of the chimney up to 45 m increases the power output of the system for a 0.2 meter chimney diameter and collector height above the ground therefore an increase in the chimney height above 45 meter causes frictional pressure drop to be higher than the driving pressure difference resulting in negative total pressure, so, optimum chimney height has been determined to be 45 meter for a fixed geometrical configuration.

iii. Increasing the collector diameter increases collector exit temperature resulting in an increased power output of the plant due to the fact that the longer air takes to reach the collector exit the more it gains heat.

iv. For the design of 30 *kw* power output optimum chimney height of 17 m and collector diameter of 17 m is selected at a 0.2 m chimney diameter and height of the collector from the ground following the economical aspect and engineering criteria. However, making any modification on the fixed parameters results in a new optimum chimney height and collector diameter.

v. The experimental data and simulated data collected has a similarities and variation throughout, the variation is a result of instability of the weather condition of the actual test site.

vi. According to the simulated result, solar chimney power plant is not economical for low power electrical power generation.

References

Backström, T. W. Von and Gannon, A. J. (2004) 'Solar chimney turbine characteristics', (March). doi: 10.1016/j.solener.2003.08.009

Backström, T. W. Von, Gannon, A. J. and Backstro, T. W. Von (2000) 'Solar Chimney Cycle Analysis With System Loss and Solar Collector Performance With System Loss and Solar', (August). doi: 10.1115/1.1314379.

Bernardes, M. A. dos S. and Zhou, X. (2013) 'On the heat storage in Solar Updraft Tower collectors - Water bags', *Solar Energy*, 91, pp. 22–31. doi: 10.1016/j.solener.2012.11.025.

Bernardes, M. A. S., Voß, A. and Weinrebe, G. (2003) 'Thermal and technical analyses of solar chimneys', 75, pp. 511–524. doi: 10.1016/j.solener.2003.09.012.

Bernardes, M. A. dos S. and Zhou, X. (2013) 'On the heat storage in Solar Updraft Tower collectors - Water bags', *Solar Energy*, 91, pp. 22–31. doi: 10.1016/j.solener.2012.11.025.

Hamdan, M. O. (2010) 'Analysis of a solar chimney power plant in the Arabian Gulf region', *Renewable Energy*. Elsevier Ltd, pp. 1–6. doi: 10.1016/j.renene.2010.05.002.

Koonsrisuk, A. and Chitsomboon, T. (2013) 'Mathematical modeling of solar chimney power plants', *Energy*. Elsevier Ltd, 51, pp. 314–322. doi: 10.1016/j.energy.2012.10.038.

Ming, T. Z., Zheng, Y., Liu, C., Liu, W., Pan, Y., Ming, T. Z., Zheng, Y., Liu, C., Liu, W. and Pan, Y. (2016) 'Simple analysis on thermal performance of solar chimney power generation systems Simple analysis

on thermal performance of solar chimney power generation systems', 9671(December). doi: 10.1179/014426009X12519696923902.

Pretorius, J. P. (2007) 'Optimization and Control of a Large-scale Solar Chimney Power Plant by', (March).

Zhou, X., Xiao, B., Liu, W., Guo, X., Yang, J. and Fan, J. (2010) 'Comparison of classical solar chimney power system and combined solar chimney system for power generation and seawater desalination', *DES*. Elsevier B.V., 250(1), pp. 249–256. doi: 10.1016/j.desal.2009.03.007.